

Elevated N1-Acetylspermidine Levels in Doxorubicin-treated MCF-7 Cancer Cells: Histone Deacetylase 10 Inhibition with an N1-Acetylspermidine Mimetic

Ajay Kumar Raj¹, Kiran Bharat Lokhande², Kratika Khunteta¹, Sachin Chakradhar Sarode³, Nilesh Kumar Sharma¹

¹Cancer and Translational Research Lab, Dr. D.Y. Patil Biotechnology & Bioinformatics Institute, Dr. D.Y. Patil Vidyapeeth,

²Bioinformatics Research Laboratory, Dr. D. Y. Patil Biotechnology and Bioinformatics Institute, Dr. D. Y. Patil Vidyapeeth,

³Department of Oral Pathology and Microbiology, Dr. D. Y. Patil Dental College and Hospital, Dr. D.Y. Patil Vidyapeeth, Pune, India

Cancer drug resistance is associated with metabolic adaptation. Cancer cells have been shown to implicate acetylated polyamines in adaptations during cell death. However, exploring the mimetic of acetylated polyamines as a potential anticancer drug is lacking. We performed intracellular metabolite profiling of human breast cancer MCF-7 cells treated with doxorubicin (DOX), a well known anticancer drug. A novel and in-house vertical tube gel electrophoresis assisted procedure followed by LC-HRMS analysis was employed to detect acetylated polyamines such as N1-acetylspermidine. We designed a mimetic N1-acetylspermidine (MINAS) which is a known substrate of histone deacetylase 10 (HDAC10). Molecular docking and molecular dynamics (MDs) simulations were used to evaluate the inhibitory potential of MINAS against HDAC10. The inhibitory potential and the ADMET profile of MINAS were compared to a known HDAC10 inhibitor Tubastatin A. N1-acetylspermidine, an acetylated form of polyamine, was detected intracellularly in MCF-7 cells treated with DOX over DMSO-treated MCF-7 cells. We designed and curated MINAS (PubChem CID 162679241). Molecular docking and MD simulations suggested the strong and comparable inhibitory potential of MINAS (−8.2 kcal/mol) to Tubastatin A (−8.4 kcal/mol). MINAS and Tubastatin A share similar binding sites on HDAC10, including Ser138, Ser140, Tyr183, and Cys184. Additionally, MINAS has a better ADMET profile compared to Tubastatin A, with a high MRTD value and lower toxicity. In conclusion, the data show that N1-acetylspermidine levels rise during DOX-induced breast cancer cell death. Additionally, MINAS, an N1-acetylspermidine mimetic compound, could be investigated as a potential anticancer drug when combined with chemotherapy like DOX.

Key Words Aantagonists and inhibitors, Doxorubicin, Epigenomics, Metabolic reprogramming, Polyamines

INTRODUCTION

Global data on cancer incidence and mortality estimated that breast cancer has exceeded lung cancer as the most commonly diagnosed cancer in women, with an estimated 2.3 million new cases (11.7%) [1].

Cancer cells have altered metabolisms compared to normal healthy cells and these alterations are responsible for their malignant properties [2,3]. Therefore, intracellular and extracellular profiles of metabolites such as polyamines, amino acids, peptides, vitamins, lipids, organic acids, carbohydrates, and nucleic acids are suggested to provide clues on metabolic adaptations during drug-induced stress in cancer cells, which accounts for their drug resistance [4-9]. Besides

a basic understanding of cancer cell metabolism, profiling of intracellular and extracellular metabolites is considered an important approach for detection of cancer based on metabolite biomarkers.

In the context of metabolic reprogramming and drug resistance, polyamines such as putrescine, spermidine, and spermine and their acetylated forms are involved in various hallmarks of cancer cells including drug resistance [10-12]. Therefore, the depletion of polyamines such as spermidine and its acetylated form N1-acetylspermidine at the intracellular levels is associated with cancer cell metabolic adaptations [10-14]. Existing data suggest that polyamine metabolites including N1-acetylspermidine are elevated in case of chemotherapy-induced cell death in cancer cells [10-14]. Due

Received March 31, 2024, Revised May 4, 2024, Accepted May 18, 2024, Published on June 30, 2024

Correspondence to Nilesh Kumar Sharma, E-mail: nilesh.sharma@dpu.edu.in, https://orcid.org/0000-0002-8774-3020



This is an Open Access article distributed under the terms of the Creative Commons Attribution Non-Commercial License, which permits unrestricted non-commercial use, distribution, and reproduction in any medium, provided the original work is properly cited.

Copyright © 2024 Korean Society of Cancer Prevention

to a lack of appropriate methodology, data is scarce to substantiate the export of acetylated forms of a polyamine such as N1-acetylspermidine in case of breast cancer cell death induced by anticancer drugs.

In recent years, the metabolic-epigenetic axis is considered a crucial pathway that may modulate the cancer metabolic landscape during drug-induced cell death [15,16]. The various classes of histone deacetylases (HDACs) are known as important pharmacological anticancer drug targets due to their implications in apoptotic cell death [16-18]. Different HDAC enzymes show distinct intracellular localization including HDAC1, -2, -3, and -8 (nucleus) and HDAC4, -5, -7, and -9 (nucleus and cytoplasm) and HDAC10 [6-10] (cytoplasm) [18,19]. Due to the specific and unique nature of HDAC10 including intracellular localization in the cytoplasm, the mechanism unleashed by HDAC10 to support the anti-apoptotic effects is mediated and linked to acetylated polyamines.

In this direction, among several epigenetic modifiers, HDAC10 is a distinct form of deacetylase that is referred to as polyamine deacetylase [17-20]. The role of HDAC10 is considered pro-tumorigenic in the context of cancer cell survival and induced drug resistance. Therefore, HDAC10 is considered a potential target for anticancer therapies by reprogramming the metabolic-epigenetic axis from pro-tumor to anti-tumor. Diminished expression and pharmacological inhibition of HDAC10 in cancer cells are associated with genomic instability and sensitization to drug insults [16,21-25].

To explore translational values of metabolic-epigenetic pathways, mimetic metabolites are conceived as anti-cancer drugs that can modulate the activity of epigenetic modifiers such as HDAC10 [26-32]. However, the idea to use a mimetic N1-acetylspermidine (MINAS) as an inhibitor of HDAC10 has not been reported previously. Based on the aforementioned knowledge, we aim to demonstrate the significance of N1-acetylspermidine in drug-induced cell death in cancer cells, specifically with regard to the anticancer drug doxorubicin (DOX). Additionally, we evaluated the inhibitory potential of MINAS against HDAC10 using molecular docking and molecular dynamics (MDs) simulations.

MATERIALS AND METHODS

Materials

Cell culture reagents including Dulbecco's Modified Eagle's Medium (DMEM) with high glucose and FBS were purchased from Invitrogen India Pvt. Ltd. and Himedia Laboratories Pvt. Ltd. MCF-7 human breast cancer cells were procured from the National Centre for Cell Science, Pune, India. Dimethyl sulfoxide (DMSO), acrylamide, DOX, and other chemicals were of molecular biology grade and obtained from Himedia Laboratories Pvt. Ltd. and Merck India Pvt. Ltd. This research was approved by the Institutional Review Board of Dr. D. Y. Patil Biotechnology and Bioinformatics Institute Pune, India (IRB/CMRAI-06082022).

Trypan blue dye exclusion assay

MCF-7 breast cancer cells were cultured and maintained in DMEM with high glucose supplemented with 10% heat-inactivated FBS and penicillin (100 units/mL)/streptomycin (100 µg/mL) at 37°C in a humidified 5% CO₂ incubator. The MCF-7 breast cancer cells were cultured at 60%–70% confluence. MCF-7 cells were plated into six-well plates at a density of 150,000 cells per well. After 16–18 hours of overnight growth, complete DMEM medium with DMSO (10 µL) solvent control and DOX (100 nM) were added in triplicate in respective wells of the six-well plate. Incubation of MCF-7 breast cancer cells was allowed for 72 hours. The morphology of cells was visualized with the help of routine phase contrast microscopy. Then, MCF-7 breast cancer cells were harvested and collected using the standard procedure. A routine trypan blue dye exclusion assay was performed to determine the viable and dead cells.

Estimation of DOX-induced apoptosis by flow cytometry

MCF-7 cells were cultured in duplicates into six-well plates at a seeding density of 1.5×10^4 cells per well. After 16–18 hours, breast cancer cells were treated with DOX (100 nM) for 72 hours along with a complete DMEM medium. The cells were then pelleted and resuspended in 1 mL of cold PBS buffer. Next, Annexin V binding buffer was added to the pellet obtained after centrifugation of MCF-7 cancer cells. The rest of the steps were followed according to the manufacturer's instructions for using the Annexin V/FITC apoptosis detection kit (ThermoFisher). Then, the recording of live and dead cells was done by BD FACSJazz Cytometer (BD Biosciences), and 10,000 events were measured for each sample [33,34].

Intracellular metabolite profiling

After completion of DOX treatment to MCF-7 breast cancer cells, cells were harvested by following the routine procedure. Three washing steps with PBS were performed to remove the traces of conditioned media. Cell pellets were suspended in hypotonic buffer (10 mM KCl, 10 mM NaCl, 20 mM Tris, pH 7.4) [35-37], and then lysed using glass homogenizer. Rest of lysis procedure was adopted from previously published procedure [35-37]. Furthermore, 250 µL of whole-cell lysate was diluted to 750 µL by adding hypotonic buffer. Whole-cell lysate (750 µL) was mixed with 250 µL 4× loading buffer (0.5 M Tris, pH 6.8, and glycerol). Next, whole cell lysate along with loading buffer was loaded on the vertical tube gel electrophoresis (VTGE) purification system (Fig. S1) with a matrix of 15% acrylamide gel (acrylamide: bisacrylamide, 30:1). The fractionated intracellular metabolites were collected in the 5× running buffer (96 mM glycine of pH at 8.3). Furthermore, liquid chromatography-high resolution mass spectrometry (LC-HRMS) analysis of VTGE-purified intracellular metabolites was carried out in a positive mode and analyzed as per the procedure adopted from the previously reported methodology

[35-37]. A detailed flow diagram of VTGE is illustrated in Figure S1.

Molecular docking

The ligand structure was downloaded from the PubChem database in expanded as structure data file format which was converted to the protein data bank (PDB) format using the PyMol software. The Protein Data Bank was used to retrieve the receptor HDAC10 protein (PDB ID: 5TD7 and PDB ID: 7KUQ) [16]. The heteroatoms were taken out from the protein before docking. Following the drag-drop step on AutoDock tool 4.2.1., the HDAC10 protein was stored [38]. After the initial steps of protein preparation, the water molecule was eliminated by selecting “edit” and “remove water molecules.” Next, the bond was corrected by assigning atoms of the AD4 type, adding polar hydrogens, and adding Kollman charges. N1-acetylspermidine (PubChem CID 496), spermidine (PubChem ID 1102), N8-acetylspermidine (PubChem ID 123689), MINAS (PubChem CID 162679241) and Tubastatin A (PubChem CID 49850262), a known HDAC10 inhibitor, were molecularly docked with the target HDAC10 protein using AutoDock Vina software [34]. For the imaging of ligand and protein complexes, the Discovery Studio Visualizer 3 (DSV3) software was used.

MDs simulations

To confirm the binding stability and strength of the complex, based on the molecular docking data, 20 ns MDs simulations for the complexes of MINAS (PubChem CID 162679241) and Tubastatin A (PubChem CID 49850262) with the structure of a HDAC10 (PDB ID: 5TD7 and PDB ID: 7KUQ) were performed with the assistance of Desmond software. Desmond has inbuilt functions to add pressure, volume system, temperature, and many functionalities to accomplish the protein-ligand binding. Molecules respectively within the cubic box of 10 Å spacing were selected using periodic boundary conditions. The conformational changes upon binding of metabolites with HDAC10 were recorded by using 1,000 trajectory frames generated during the 20 ns MD simulation and the root mean square deviation (RMSD) was calculated to reveal the binding with HDAC10.

The steepest descent method was used to minimize the complex system energetically with the OPLS-2005 force field. The 20 ns time scale MD simulations for each complex were performed at a constant NPT (N, number of atoms; P, pressure; T, temperature) ensemble. Throughout the equilibrations, systems were coupled with the Martyna–Tobias–Klein barostat method for controlling pressure at 1 atm, and the temperature was regulated by using the velocity rescaling Nose Hoover chain thermostat method at 300 K. The M-SHAKE algorithm was used to constrain the bond length of hydrogen atoms. The cut-off for short-range electrostatics and van der Waals interactions is maintained at 1 nm. Also, the long-range Coulomb electrostatic interactions were cal-

ibrated through particle mesh Ewald summation. The leap-frog algorithm was used to compute the equation of motion with a time step stamp of 2 fs. The conformational changes in HDAC C- α backbone atoms after the binding of metabolites were compared with the initial conformations of HDAC10 in terms of RMSD. Also, the fluctuations in the amino acids of HDAC10 after binding of the ligands such as MINAS and Tubastatin A were computed using the trajectories generated during the 10 ns MD simulation and presented as a root mean square fluctuation (RMSF) graph.

Toxicity prediction

MINAS and Tubastatin A were tested for drug-induced liver injury, a substrate of P-glycoprotein (P-gp), cell toxicity, carcinogenicity, maximal recommended therapeutic dose (MRTD), and druglikeness using vNN-ADMET and SWISS-ADMET web servers [39,40].

Statistical analysis

The experiments were independently conducted three times. The results are expressed as the mean \pm SD. Data were statistically analyzed in Microsoft Excel statistical package (Microsoft) using the student's *t*-test. Statistical significance was accepted at a level of $P < 0.05$.

RESULTS

The heightened status of polyamines metabolism is linked to the tumor hallmarks including high proliferation and drug resistance in breast cancer cells [5-10]. Given the importance of polyamines in the metabolic-epigenomic landscape, acetylated polyamines such as N1-acetylspermidine and N1-acetylputrescine are thought to be intracellular indicators of drug-induced stress and death in cancer cell growth and proliferation [11-14].

As a result, it is proposed that the elevation of intracellular polyamines and their acetylated forms may serve as metabolite biomarkers in breast cancer cells treated by an anticancer drug such as DOX. At the same time, an idea to explore mimetic of acetylated polyamines is significantly lacking that could potentiate the DOX mediated cancer cell death.

Intracellular metabolite profiling

We used DOX as a source of anticancer drug compositions to explore the intracellular metabolites of breast cancer cells under drug-induced cell death. A simple and routine trypan blue dye exclusion assay was performed to demonstrate DOX-mediated cell death in MCF-7 breast cancer cells. The microscopy photographs revealed that compared with the DMSO control (Fig. 1A), there was pronounced death and loss of viability of MCF-7 cells treated with DOX (Fig. 1B). Quantitative data indicated a clear and profound decrease in the total number of MCF-7 cells due to DOX treatment over the DMSO control (Fig. 1C). Concomitantly, data showed a

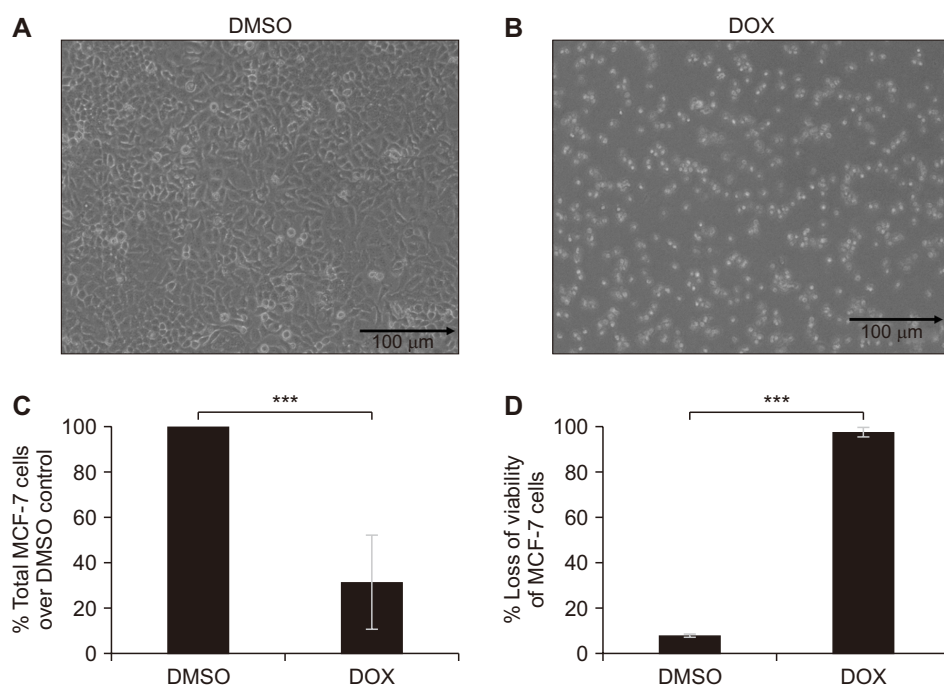


Figure 1. Doxorubicin (DOX) induces loss of cell viability in MCF-7 breast cancer cells. (A) MCF-7 breast cancer cells were treated by dimethyl sulfoxide (DMSO) and DOX (100 nM) for 72 hours. Routine microscopy was performed at 100 \times to observe the cell number and cellular morphology. (B) MCF-7 cancer cells were treated by DMSO and DOX (100 nM) for 72 hours. The trypan blue dye exclusion assay was performed to estimate the percentage of viable and dead cells. Data are represented as mean \pm SD. Each experiment was conducted independently three times. ***Significantly different from the DMSO control at the P -value \leq 0.001.

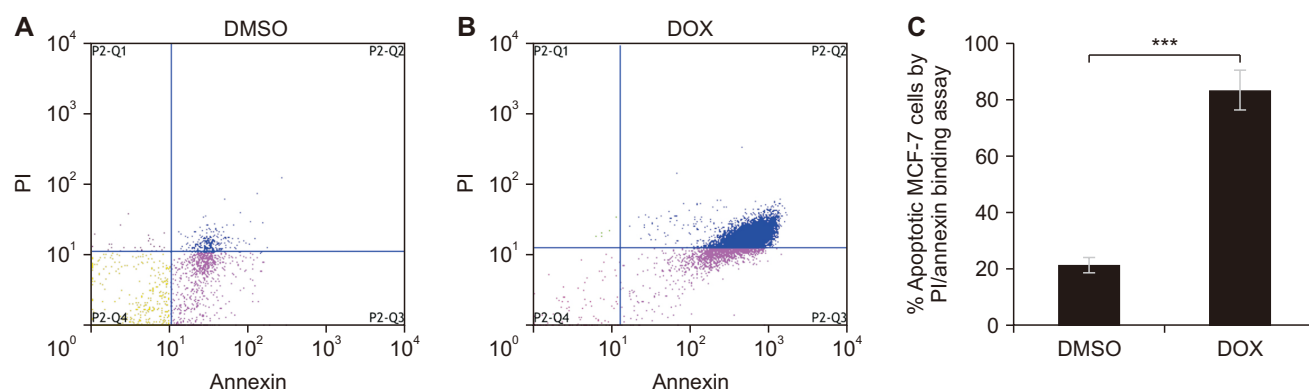


Figure 2. Doxorubicin (DOX) treatment for MCF-7 breast cancer cells displays apoptotic cell death. MCF-7 cancer cells were treated with dimethyl sulfoxide (DMSO) and DOX (100 nM) for 72 hours. At the end of treatment, harvested MCF-7 cells were subjected to PI/annexin V staining and analyzed by a flow cytometer. The scatter plots of cells were stained with PI and Annexin V conjugated with FITC for analysis of apoptotic cells in MCF-7 breast cancer cells. (A) DMSO control, (B) DOX. (C) The percentage of apoptotic cells was calculated based on the number of cells in quadrants 3 and 4 stained with Annexin V and PI divided by the total number of cells. Data are represented as mean \pm SD. Each experiment was conducted independently three times. ***Significantly different from the DMSO control at a P -value \leq 0.001.

significant loss of more than 90% in DOX treated MCF-7 cells compared to the DMSO control (Fig. 1D).

We performed a PI-Annexin V staining assay to evaluate the extent of apoptosis in MCF-7 cancer cells. Data collected from the flow cytometer indicated a significant increase in the Q2-gated MCF-7 cell population upon DOX treatment (Fig. 2A) compared to the DMSO control (Fig. 2B). The bar graph of the percentage of apoptotic MCF-7 cancer cells treated with DOX is more than 80% over DMSO control (Fig. 2C). It is important to note that the efficacy of DOX in MCF-7 cancer cells is well-known, and our observations are in line with existing views. An approach to explore alterations in intracellular

metabolites specifically in the context of acetylated polyamines is crucial, and DOX-treated MCF-7 cancer cells are used as one of the suitable study models.

Intracellular lysates of MCF-7 cells treated by DMSO and DOX were purified by a novel and in-house VTGE tool and analyzed by LC-HRMS. Literature hints that the detection of intracellular polyamines and their acetylated forms at the intracellular level is faced with sensitivity issues due to relatively low concentrations of polyamines. However, we showed the strikingly elevated presence of N1-acetylspermidine in the case of DOX-treated breast cancer cells over the DMSO control; the MS and MS/MS spectra in +ESI mode were ex-

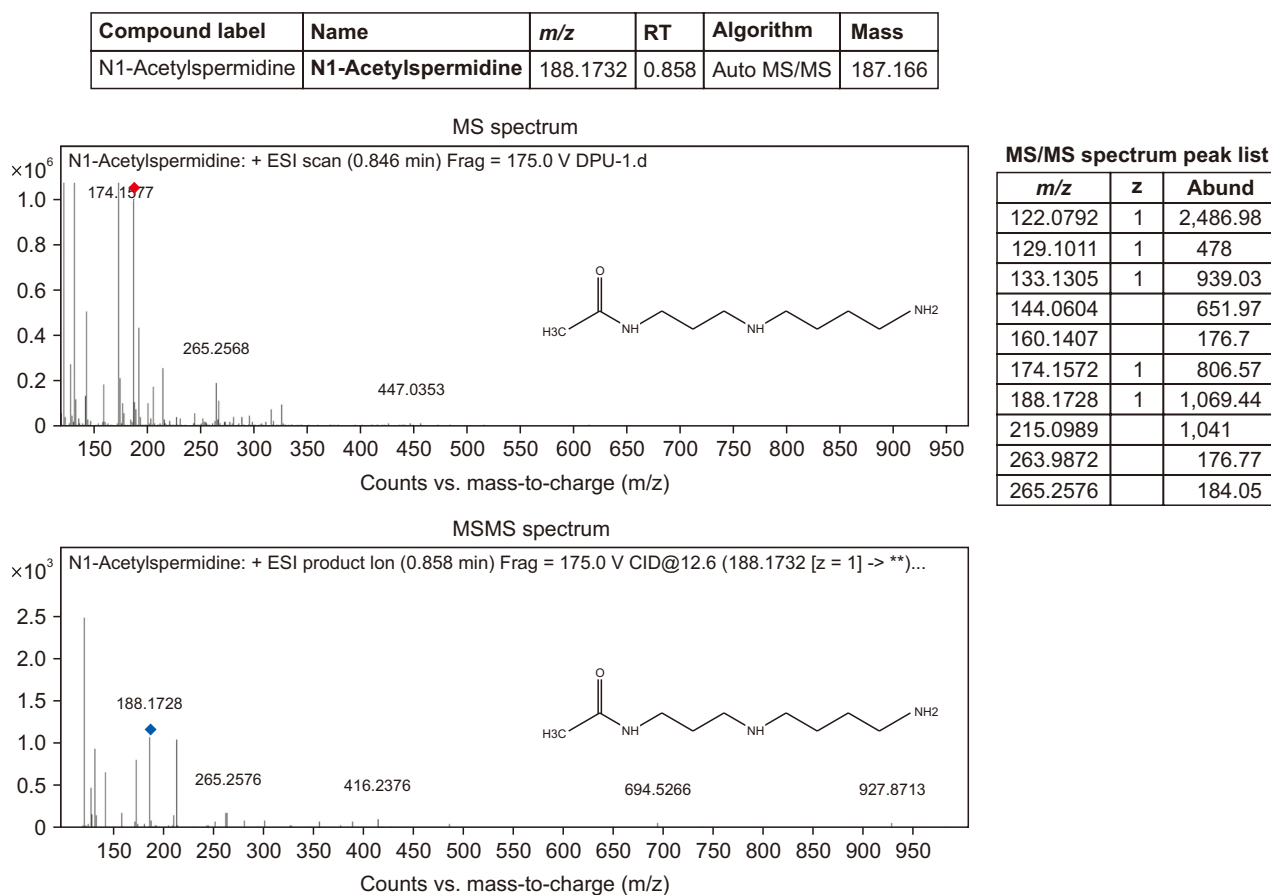


Figure 3. The levels of N1-acetylspermidine is elevated in MCF-7 breast cancer cells treated with doxorubicin (DOX). Intracellular metabolite profiling of MCF-7 cancer cells treated with DOX is assisted by vertical tube gel electrophoresis and liquid chromatography-high resolution mass spectrometry (LC-HRMS). MS and MS/MS derived product ion spectra of N1-acetylspermidine were collected in the positive electrospray ionization (ESI) mode.

tracted from LC-HRMS of purified intracellular lysates (Fig. 3). Product ion spectra of N1-acetylspermidine (m/z 188.1732, RT-0.838, mass-187.166) in the +ESI mode showed the presence of characteristic mass ions such as 144.0604, 174.1577, 188.1728, and 265.2568 (Fig. 3).

The identified acetylated polyamine N1-acetylspermidine is highly convincing in terms of metabolite characteristics and abundance in the case of DOX-treated MCF-7 cancer cells. As a piece of evidence, intracellular metabolite profiling showed the accumulation of an aglycan form of DOX as adriamycinone in MCF-7 cancer cells treated with DOX (Fig. 4). It is expected that DOX-treated MCF-7 cancer cells will have the intracellular abundance of DOX and its metabolized products such as adriamycinone (m/z -419.082, RT-17.103, mass-414.1034). The observed intracellular adriamycinone in MCF-7 cancer cells showed desired +ESI product ions such as 230.1370, 326.0276, and 419.0820.

Previously, we have employed the standardized in-house VTGE-assisted methodology for the profiling of intracellular metabolites of cancer cells treated by anticancer drugs and compositions such as DOX, CUDF, and GUDF [32,35-37].

In the present study, we have extended the observations of DOX-induced cell death in breast cancer cells with the potential metabolic adaptations in the form of intracellular acetylated forms of polyamines.

This paper warrants further investigations to employ different cancer cells and anticancer drugs that may involve alterations of acetylated polyamines as metabolic adaptations in response to drug-induced cell death. Based on the above observations and premises, we explored the biological relevance of intracellular acetylated polyamines such as N1-acetylspermidine and MINAS as a potential inhibitor of HDAC10 and eventually a future candidate that can promote cell death in breast cancer cells.

Molecular docking

After identification of intracellular acetylated polyamines in DOX-treated MCF-7 breast cancer, we further asked questions about the relevance of elevated levels of N1-acetylspermidine in anticancer drug-induced cell death in breast cancer cells. To answer this question, we initially performed molecular docking to know the binding affinity and molecular

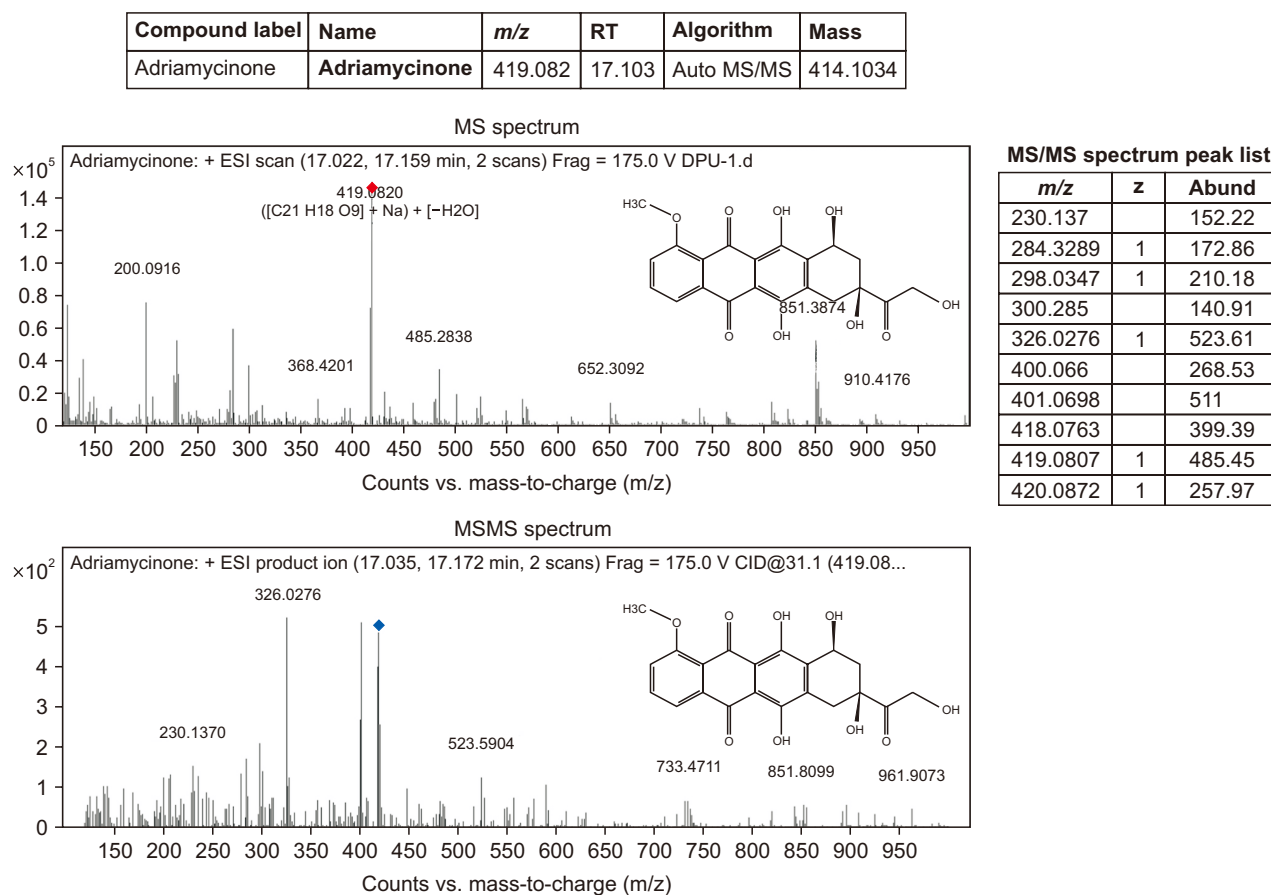


Figure 4. Doxorubicinone, an aglycan form of doxorubicin (DOX), is present in DOX-treated MCF-7 breast cancer cells. Intracellular metabolite profiling of MCF-7 cancer cells treated by DOX is assisted by vertical tube gel electrophoresis and liquid chromatography-high resolution mass spectrometry (LC-HRMS). MS and MS/MS-derived product ion spectra of doxorubicinone were collected in the positive electrospray ionization (ESI) mode. RT, retention time.

interactions with a known polyamine deacetylase HDAC10. Molecular docking and DSV3 indicated that N1-acetylspermidine (−6.5 kcal/mol) showed comparatively higher binding affinity and more importantly, interactions with amino acid residues ranging from His136-Ser141 (Fig. S2, Tables 1, 2) were seen. The binding of N1-acetylspermidine within the catalytic residues of HDAC10 is supported by the presence of conventional hydrogen bonds with amino acid residues such as Ala24, His136, and Asp174.

This observation encouraged the design of MINAS as a potential inhibitor of HDAC10. Initially, we screened for various designs of a MINAS (Table S1). By considering various parameters such as binding affinity (Table S2), interacting inhibitory amino acid residues, and ADMET profiles (Table S3), we focused on a potential MINAS compound that was submitted to PubChem for curation, and a PubChem ID: 162679241 was received (Table 2). Molecular docking and visualization data suggest that the binding affinity of MINAS (−8.2 kcal/mol) is significantly comparable to a known HDAC10 inhibitor Tubastatin A (−8.4 kcal/mol). Detailed mo-

Table 1. Among various polyamines, N1-acetylspermidine displays high binding affinity for HDAC10

Sr. No.	Name of polyamines/ligands	Binding energy (−kcal/mol)	RMSD (value l.b.)	RMSD (value u.b.)
1	N1-Acetylspermidine (PubChem CID 496)	−6.5	0.000	0.000
2	Spermidine (PubChem ID 1102)	−5.7	0.000	0.000
3.	N1-Acetylputrescine (PubChem ID 122356)	4.7	0.000	0.000
4	N8-Acetylspermidine (PubChem ID 123689)	4.9	0.000	0.000

These polyamines including N1-acetylspermidine are detected at the intracellular and extracellular levels and studied with the help of AutoDock Vina. HDAC10, histone deacetylase 10; RMSD, root mean square deviation; l.b., lower bound; u.b., upper bound.

Table 2. Mimetic N1-acetylspermidine is predicted as an inhibitor of HDAC10

Sr. No.	Name of polyamines/ligands	Binding energy (–kcal/mol)	Inhibitory site binding residues	No. of H-bonds	Distance of H-bonds (Å)
1	N1-Acetylspermidine (PubChem CID 496)	–6.5	Ala24 Asp174 His136	3	2.00 2.0 2.16
2	MINAS (PubChem CID 162679241)	–8.2	Cys184 Tyr183 Ser140 Ser141 Gln139	5	2.00 2.0 3.15 2.09 2.5
3.	Tubastatin A (PubChem CID 49850262) (a known inhibitor of HDAC10)	–8.4	Ser138 Ser140 Tyr183 Cys184	4	3.02 1.2 2.10 2.17

The binding affinity and nature of inhibitory site amino acid residues are analyzed with the help of AutoDock Vina and Discovery Studio software. HDAC10, histone deacetylase 10; MINAS, mimetic N1-acetylspermidine; H-bonds, hydrogen bonds.

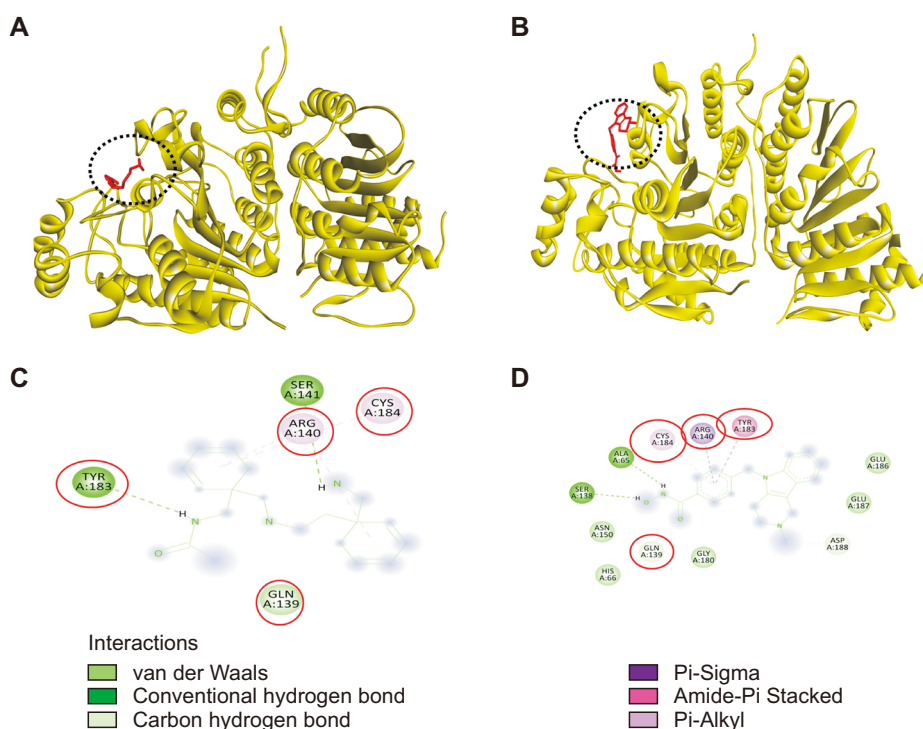


Figure 5. Mimetic N1-acetylspermidine (MINAS) shows strong binding to the inhibitory site of histone deacetylase 10 (HDAC10) and is highly comparable to a known inhibitor Tubastatin A. Molecular docking and inhibitory interaction by MINAS and Tubastatin A against HDAC10 were studied with the help of AutoDock Vina. (A) A ribbon structure with a full three-dimensional (3D) view between MINAS and HDAC10. (B) A ribbon structure with a full 3D view between Tubastatin A and HDAC10. (C) Discovery Studio Visualizer assisted 2D image of docked molecular structure between MINAS and HDAC10. (D) Discovery Studio Visualizer assisted 2D image of docked molecular structure between Tubastatin A and HDAC10.

molecular interaction showed an overlapping inhibitory binding pocket between MINAS (Fig. 5A) and Tubastatin A (Fig. 5B). Data also indicate key inhibitory amino acid residues including His136, Gln139 Ser140, Ser141, Tyr183, and Cys184 are shared between MINAS (Fig. 5C) and a known HDAC10 inhibitor Tubastatin A (Fig. 5D). The nature and number of interacting bonds including hydrogen bonds, van der Waals, and alkyl interactions are found to be similar between MINAS and Tubastatin A (Table 2).

Further, we performed MD simulations of MINAS and Tubastatin A with HDAC10 for the evaluation of the stability of the complex. A 20 ns RMSD plot obtained for MINAS and Tubastatin A against HDAC10 revealed similar RMSD val-

ues in the range of 1–3 Å. At the end of the simulation, the RMSD values remained stable for both MINAS and Tubastatin A (Fig. 6). RMSD plot hints at the stable complex between MINAS and HDAC10 and is almost similar to a known HDAC10 inhibitor Tubastatin A. Additionally, a comparison of the RMSF plot of MINAS and Tubastatin A revealed minimal fluctuations within the desirable range of inhibitory amino acid residues (120–200) of HDAC10 during simulations. This suggested the strong and stable complex between MINAS and HDAC10, and RMSF plot was similar to Tubastatin A (Fig. 7).

We compared the ligand-protein contact maps of MINAS (Fig. 8A) and Tubastatin A (Fig. 8B) with HDAC10, and the data indicated similar ligand contact maps with specific

amino acid residues notably Glu24, Asn93, His136, His137, Trp205, PRO Pro207, and GLU Glu274. The range for amino acid residues interaction fraction is estimated from 0.0 to 0.6 scales for both MINAS and Tubastatin A (Fig. 8). Altogether, MINAS and Tubastatin A appear to share a similar inhibitory binding pocket with identical binding affinity and protein complex.

ADMET profiling

Furthermore, we intended to know the ADMET profile and

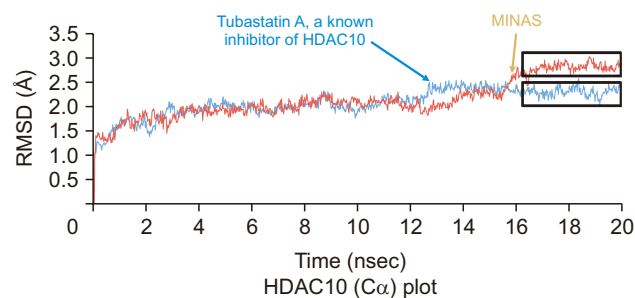


Figure 6. Mimetic N1-acetylspermidine (MINAS) and Tubastatin A show similar and stable inhibitory complex within acceptable root mean square deviation (RMSD) values. MD simulations for 20 ns derived RMSD plot of histone deacetylase 10 (HDAC10) in complex with MINAS and Tubastatin A.

druglikeness and its comparison with Tubastatin A. ADMET data indicate that MINAS has certain advantages in terms of the high MRTD value, lack of liver toxicity, lack of affinity to P-gp transporter and the negative mutagenicity in the Ames test over Tubastatin A (Fig. 9). Evaluation of MINAS for druglikeness is encouraging with a bioavailability score of 0.55 and no violations for various parameters including Lipinski (Fig. S3). In summary, the ADMET and druglikeness profile of MINAS is favorable for the future possibilities of exploration as an HDAC10 inhibitor and a good candidate for anticancer agents.

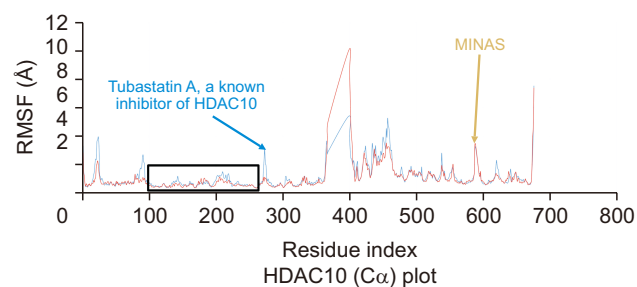


Figure 7. Mimetic N1-acetylspermidine (MINAS) and Tubastatin A display minimal fluctuations of protein complex. Molecular dynamics simulations for 20 ns derived root mean square fluctuation (RMSF) plot of histone deacetylase 10 (HDAC10) in complex with MINAS and Tubastatin A.

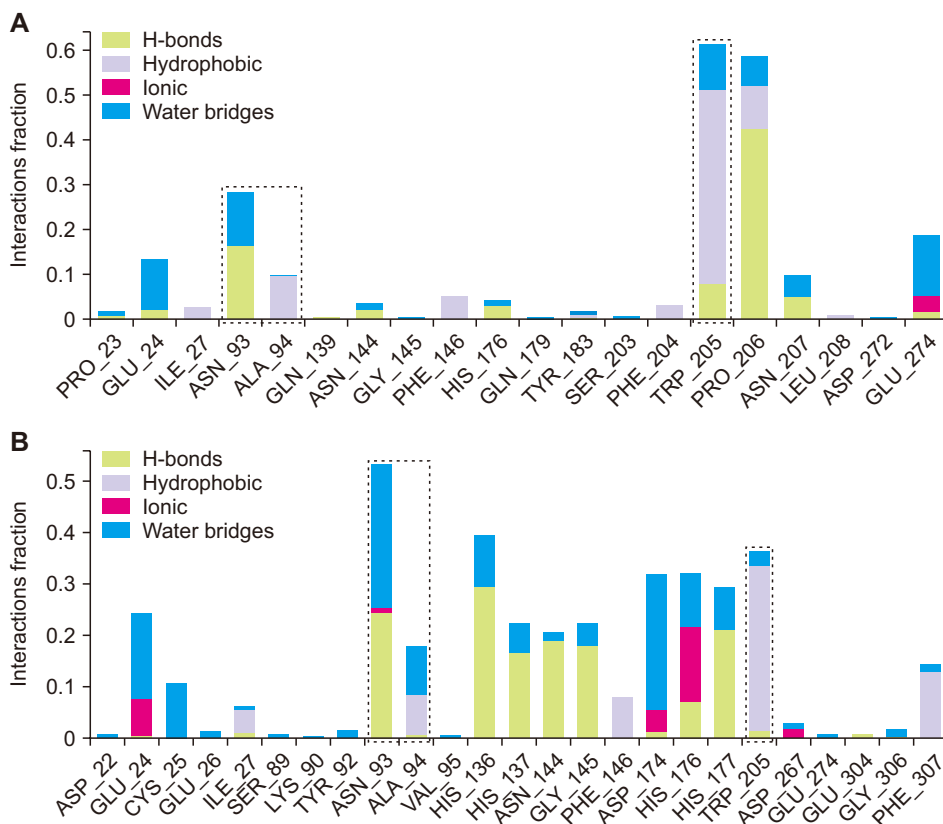


Figure 8. Protein-ligand contact map of mimetic N1-acetylspermidine (MINAS) and Tubastatin A within the inhibitory residues of histone deacetylase 10 (HDAC10). Molecular dynamics simulations for 20 ns derived protein-ligand contact map of HDAC10 in complex with (A) MINAS and (B) Tubastatin A. H-bonds, hydrogen bonds.

Mimetic N1-acetylspermidine (MINAS)
PubChem CID: 162679241

Query	Liver Toxicity		Metabolism						Membrane Transporters				Others		MRTD (mg/day)
	DILI	Cyto-toxicity	HLM	1A2	3A4	2D6	2C9	2C19	BBB	P-gp Inhibitor	P-gp Substrate	hERG Blocker	MMP	AMES	
	No	No	Yes	No	No	No	No	No	No	No	No	No	No	No	315

Tubastatin A (a known inhibitor of HDAC10)
PubChem CID: 49850262

Query	Liver Toxicity		Metabolism						Membrane Transporters				Others		MRTD (mg/day)
	DILI	Cyto-toxicity	HLM	1A2	3A4	2D6	2C9	2C19	BBB	P-gp Inhibitor	P-gp Substrate	hERG Blocker	MMP	AMES	
	Yes	No	Yes	No	No	Yes	No	No	No	Yes	Yes	Yes	No	Yes	132

Figure 9. Reduced drug-induced liver injury and cytotoxicity by a mimetic N1-acetylspermidine (MINAS) over Tubastatin A. ADMET profile is generated using vNN-ADMET server. (A) MINAS and (B) Tubastatin A.

DISCUSSION

In the context of various types of malignancies including breast cancer, altered levels of polyamines and their acetylated forms are noticed at the intracellular levels and extracellular environment including biological fluids such as serum and urine [5-14]. There is limited cell-based, in vivo, and clinical data on the nature and extent of the abundance of polyamines and their acetylated products including N1-acetylspermidine and N1-acetylputrescine in the context of drug-induced cell death in breast cancer cells.

Moreover, identifications of polyamines and their acetylated forms such as N1-acetylspermidine and N1-acetylputrescine are related to the metabolically driven epigenetic landscape of cancer cells during various stresses including drug-induced cell death [10-14]. The exploration of polyamines and their acetylated forms including N1-acetylspermidine and N1-acetylputrescine is encouraged to develop mimetics of these acetylated polyamines as inhibitors of the key enzyme HDAC10 that play an important role in the metabolisms of cancer cells.

In this study, we have shown the clear abundance of N1-acetylspermidine in the intracellular compartment of MCF-7 breast cancer cells treated with DOX. The antiproliferative and pro-cell death effects of DOX have been reported earlier [35,36]. The novelty of this study extends beyond the ability of DOX to cause cell death in MCF-7 cancer cells. In reality, DOX-induced cell death in MCF-7 cancer cells is just one model used to investigate the significance of intracellular polyamines and their acetylated forms in the context of cell death, as well as the implications with HDAC10.

Importantly, the biological relevance of polyamines and their acetylated forms such as N1-acetylspermidine and N1-acetylputrescine is well supported by in vitro and preclinical evidence on the secretion of polyamines and acetylated forms in the cells, tissues, and biological fluids [10-14]. Previous studies have provided insights into the relevance of high levels of N1-acetylated derivatives of spermidine and spermine in various types of tumors including breast and col-

orectal cancer [10-14]. However, normal tissues are found to contain lower amounts of N1-acetylated derivatives of spermidine and spermine compared to tumor tissues. Considering this, the significance of N1-acetylspermidine detection at intracellular levels and their secretion into extracellular fluids could serve as markers for drug responsiveness in cellular, preclinical, and clinical models. In other words, elevated levels of N1-acetylspermidine could be a potential indicator for drug-induced cell death in breast cancer cells.

Besides the relevance of intracellular N1-acetylspermidine in breast cancer cell death, the molecular interactions of N1-acetylspermidine, N1-acetylputrescine, and polyamines provided a clue on the efficient binding of N1-acetylspermidine within the catalytic residues of HDAC10, a form of polyamine deacetylase [15,16]. In the literature, sufficient views support the link between N1-acetylspermidine and HDAC10 [17-20]. At the same time, HDAC10 is reported as the pro-cancer cytoplasmic protein that creates a favorable metabolic-epigenomic landscape for cancer cells' growth and proliferation. Therefore, data supporting the molecular interactions of N1-acetylspermidine with HDAC10 clued for the potential design of MINAS against HDAC10 which can be a potential inhibitor. Molecular docking and MD simulations indicated the strong and stable complex with HDAC10 inhibitory site. Prominent amino acid residues including Glu24, Asn93, His136, His137, Trp205, Pro207, and Glu274 complexed by MINAS overlapped with the inhibitory complex by a known inhibitor Tubastatin A [16,21-24]. Tubastatin A, piperidine-4-acrylhydroxamates, and forms of pharmacological inhibitors are reported as selective inhibitor against HDAC10 that forms a molecular complex in the same amino acid residues such as Glu24, Asn93, His136, His137, Trp205, Pro207, and Glu274 [24-32].

Recent structural studies revealed the importance of catalytic amino acid residues such as His136 and His137 in the interaction of acetylated polyamines such as N1-acetylspermidine with HDAC10 [16,21-24]. In other ways, interacting amino acid residues including His136 and His137 could be instrumental in the evaluation of potent inhibitors of HDAC10.

In a similar context, MINAS showed strong binding to the inhibitory pocket residues such as His136 and His137. Therefore, MINAS could be explored as a potential anticancer agent.

Some selective inhibitors of HDAC10 including Tubastatin A, MC1575, MC1568, and hydroxamic acid derivatives have been alleviate resistance to chemotherapeutic drugs, suggesting their potential as combinatorial anticancer agents [24-32]. Such observations support the claim of our paper on the relevance of MINAS, a new class of an HDAC10 inhibitor, similar to others including Tubastatin A. In other ways, specific inhibitors of HDAC10 and other class II HDACs are potential candidates for future combinatorial classes of anticancer drugs.

The RMSD and RMSF pattern's compelling similarity to that of a popular HDAC10 inhibitor Tubastatin A is noteworthy. Based on recent clinical data, pieces of evidence suggest that polyamines play a role in mitochondria-based apoptotic death of cancer cells [28-32]. Tubastatin A, an HDAC10 inhibitor, has pro-cancer cell death effects. Therefore, the potential of MINAS as an HDAC10 inhibitor could be linked to the current understanding that combinatorial treatment could be a better avenue for certain cancer cells with altered polyamine metabolism. The future scope of MINAS falls in the current needs of reduction of doses of cytotoxic drugs and achieving combinatorial drug treatment through the use of metabolite mimics like MINAS.

It is suggested that a significant intracellular buildup of N1-acetylspermidine and N1-acetylputrescine could be a potential metabolic environment for cancer cells under stress [10-14]. The possibility of breast cancer cells exporting acetylated polyamines to an extracellular milieu may be considered from therapeutic and diagnostic perspectives. Another proposition is that the elevation of an intracellular and extracellular pool of acetylated polyamines may reduce the pool of acetyl-CoA intracellularly and could be favorable metabolic adaptations by breast cancer cells during drug-induced stress. In our study, molecular and MD simulations indicate that N1-acetylspermidine can occupy the inhibitory binding pocket of HDAC10. This observation led to the idea of designing MINAS as a potential inhibitor of HDAC10. Hence, the implications of MINAS as an inhibitor of HDAC10 are compatible with the current efforts by highlighting the relevance of HDAC10 inhibitors in cancer therapeutics [29]. Some findings link the role of polyamines in mitochondria-based pro-apoptotic death in cancer cells [41-43]. Future work will be necessary to explore the link between the intracellular level of N1-acetylspermidine and mitochondrial functionality during drug-induced cell death.

A recent study highlighted the relevance of elevated levels of acetylated polyamines such as diacetylspermine and N1-acetylspermdime in the case of DOX-treated TNBC patient-derived xenograft models. Besides breast cancer, the significance of acetylated forms of polyamines such as

N1-acetylspermidine is linked with non-small-cell lung cancer and colorectal cancer [44-49]. Our observation of the elevated intracellular presence of N1-acetylspermidine in DOX-treated breast cancer cells is in line with the existing views of drug-induced metabolic adaptations and polyamines.

The role of SAT1 has been explored in the drug-induced metabolic adaptations in breast cancer cells [46-50]. Conversely, tumor suppressor SAT1, known for the acetylation of polyamines such as spermidine, could be implicated in drug-induced cell death in cancer cells [44-49]. In this way, an abundance of SAT1 and SAT1-catalyzed polyamine products such as N1-acetylspermidine could be an indicator of reduced proliferation and drug-induced cell death. Our observations suggest the same proposition that DOX treatment could have induced metabolic reprogramming by activating the expression of SAT1, and this could lead to the elevation of intracellular levels of N1-acetylspermidine in breast cancer cells compared to DMSO control.

Additionally, analogs of polyamines such as N1, N11-diethylnorspermine (DENSpm) are reported to induce apoptosis in melanoma, breast, prostate, and colon cancer cells [50,51]. In essence, various enzymes that regulate the polyamine-epigenetic axis are shown as potential anticancer targets [51]. Polyamine analogs are explored for their ability to inhibit various deacetylases and demethylases and these analogs are considered one of the new forms of anticancer agents [52-56]. Hence, MINAS as an inhibitor of HDAC10 could be a valuable combinatorial approach in chemotherapy-induced cell death.

A relevant question is raised regarding the toxicity and

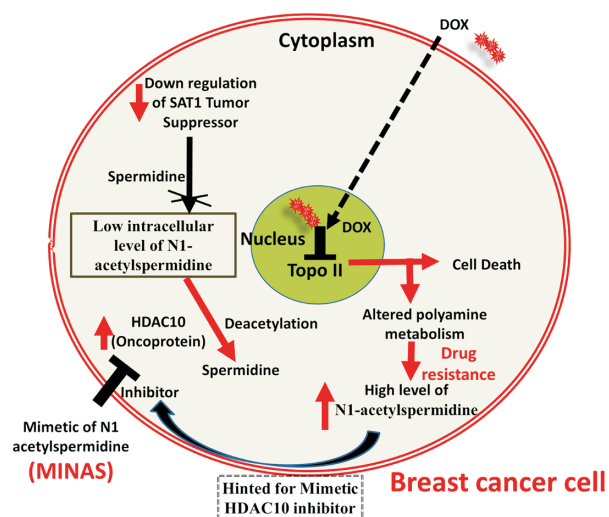


Figure 10. A proposed model on the role of acetylated polyamines in drug-induced cell death in cancer cells. A mimetic N1-acetylspermidine (MINAS) is illustrated as an inhibitor of histone deacetylase 10 (HDAC10), and its potential role in cancer cell death is proposed. DOX, doxorubicin.

other drug characteristics profile of MINAS. To address these concerns, vNN-ADMET and SWISS-ADMET prediction web servers were employed, and the results suggested that MINAS did not have liver toxicity or carcinogenicity and it is not a substrate of the P-gp transporter. It's crucial to note that MINAS performs substantially better in terms of toxicity and other drug candidate profiles than Tubastatin A, a well-known HDAC10 inhibitor.

The potential applications of MINAS at preclinical and clinical levels for cancer patients could be exploited as a component of combinatorial treatment options along with a low dose of conventional chemotherapy drugs. Majority of chemotherapy drugs at a high dose are known to display noticeable side effects such as cardiotoxicity and muscle weakness. Therefore, MINAS along with conventional anticancer drugs could be a better option to achieve desired cancer cell death and at the same time less side effects. A flow model on the relevance of MINAS in drug-induced cell death in breast cancer cells is presented (Fig. 10).

In conclusion, this study provides evidence for elevated intracellular levels of N1-acetylspermidine in breast cancer cells undergoing drug-induced cell death. Based on the importance of N1-acetylspermidine in this process, we designed MINAS, a potential inhibitor of HDAC10, using molecular docking and MD simulations. Our results demonstrate that MINAS forms stable complexes with HDAC10 with binding affinity similar to that of the known inhibitor, Tubastatin A. Moreover, MINAS exhibits better characteristics such as lower toxicity, higher MRTD value, and improved druglikeness compared to Tubastatin A. These findings suggest that MINAS may be a promising anticancer drug candidate that can modulate HDAC10. The study also proposes the exploration of intracellular metabolite profiling, specifically the levels of acetylated polyamines such as N1-acetylspermidine, as indirect evidence of DOX-induced cell death in breast cancer cells. We suggest that N1-acetylspermidine could act as a modulator of the metabolic-epigenomic axis in cancer cells, affecting their survival and response to drug-induced stress. Acetylated polyamines may also serve as biomarkers to assess drug responsiveness in breast cancer patients, and mimetics of acetylated polyamines could potentially be used in combinatorial anticancer approaches.

ACKNOWLEDGMENTS

The authors acknowledge facilities and support from DST-FIST sponsored research lab, Central Research Facility (DPU, Pune) and SAIF, IIT, Mumbai, India.

FUNDING

Intramural funding from Dr. D. Y. Patil Vidyapeeth, Pune (grant no: DPU/01/12/2020).

CONFLICTS OF INTEREST

No potential conflicts of interest were disclosed.

SUPPLEMENTARY MATERIALS

Supplementary materials can be found via <https://doi.org/10.15430/JCP.24.002>.

ORCID

Ajay Kumar Raj, <https://orcid.org/0000-0001-7690-1284>
 Kiran Bharat Lokhande, <https://orcid.org/0000-0001-6945-8288>
 Kratika Khunteta, <https://orcid.org/0000-0002-7912-8431>
 Sachin Chakradhar Sarode, <https://orcid.org/0000-0003-1856-0957>
 Nilesh Kumar Sharma, <https://orcid.org/0000-0002-8774-3020>

REFERENCES

- Sung H, Ferlay J, Siegel RL, Laversanne M, Soerjomataram I, Jemal A, et al. Global cancer statistics 2020: GLOBOCAN estimates of incidence and mortality worldwide for 36 cancers in 185 countries. *CA Cancer J Clin* 2021;71:209-49.
- Qiu S, Cai Y, Yao H, Lin C, Xie Y, Tang S, et al. Small molecule metabolites: discovery of biomarkers and therapeutic targets. *Signal Transduct Target Ther* 2023;8:132.
- Hanahan D, Weinberg RA. Hallmarks of cancer: the next generation. *Cell* 2011;144:646-74.
- Xiao Y, Yu TJ, Xu Y, Ding R, Wang YP, Jiang YZ, et al. Emerging therapies in cancer metabolism. *Cell Metab* 2023;35:1283-303.
- Halma MTJ, Tuszynski JA, Marik PE. Cancer metabolism as a therapeutic target and review of interventions. *Nutrients* 2023;15:4245.
- Patra S, Elahi N, Armorer A, Arunachalam S, Omala J, Hamid I, et al. Mechanisms governing metabolic heterogeneity in breast cancer and other tumors. *Front Oncol* 2021;11:700629.
- Corchado-Cobos R, García-Sancho N, Mendiburu-Eliçabe M, Gómez-Vecino A, Jiménez-Navas A, Pérez-Baena MJ, et al. Pathophysiological integration of metabolic reprogramming in breast cancer. *Cancers (Basel)* 2022;14:322.
- Navarro C, Ortega Á, Santeliz R, Garrido B, Chacín M, Galban N, et al. Metabolic reprogramming in cancer cells: emerging molecular mechanisms and novel therapeutic approaches. *Pharmaceutics* 2022;14:1303.
- Guo L, Lee YT, Zhou Y, Huang Y. Targeting epigenetic regulatory machinery to overcome cancer therapy resistance. *Semin Cancer Biol* 2022;32:487-502.
- Casero RA Jr, Murray Stewart T, Pegg AE. Polyamine metabolism and cancer: treatments, challenges and opportunities. *Nat Rev Cancer* 2018;18:681-95.
- Gerner EW, Bruckheimer E, Cohen A. Cancer pharmacoprevention: targeting polyamine metabolism to manage risk factors for colon cancer. *J Biol Chem* 2018;293:18770-8.
- Lee YR, Lee JW, Hong J, Chung BC. Simultaneous deter-

- mination of polyamines and steroids in human serum from breast cancer patients using liquid chromatography-tandem mass spectrometry. *Molecules* 2021;26:1153.
13. Persson L, Rosengren E. Increased formation of N1-acetylspermidine in human breast cancer. *Cancer Lett* 1989;45: 83-6.
 14. Holbert CE, Cullen MT, Casero RA Jr, Stewart TM. Polyamines in cancer: integrating organismal metabolism and antitumor immunity. *Nat Rev Cancer* 2022;22:467-80.
 15. Duong V, Bret C, Altucci L, Mai A, Duraffourd C, Loubersac J, et al. Specific activity of class II histone deacetylases in human breast cancer cells. *Mol Cancer Res* 2008;6:1908-19.
 16. Hai Y, Shinsky SA, Porter NJ, Christianson DW. Histone deacetylase 10 structure and molecular function as a polyamine deacetylase. *Nat Commun* 2017;8:15368.
 17. Li Y, Zhang X, Zhu S, Dejene EA, Peng W, Sepulveda A, et al. HDAC10 regulates cancer stem-like cell properties in KRAS-driven lung adenocarcinoma. *Cancer Res* 2020;80:3265-78.
 18. Cheng F, Zheng B, Wang J, Zhao G, Yao Z, Niu Z, et al. Histone deacetylase 10, a potential epigenetic target for therapy. *Biosci Rep* 2021;41:BSR20210462.
 19. Zhang T, Wang Z, Liu M, Liu L, Yang X, Zhang Y, et al. Acetylation dependent translocation of EWSR1 regulates CHK2 alternative splicing in response to DNA damage. *Oncogene* 2022;41:3694-704.
 20. Tavares MO, Milan TM, Bighetti-Trevisan RL, Leopoldino AM, de Almeida LO. Pharmacological inhibition of HDAC6 overcomes cisplatin chemoresistance by targeting cancer stem cells in oral squamous cell carcinoma. *J Oral Pathol Med* 2022;51:529-37.
 21. Guardiola AR, Yao TP. Molecular cloning and characterization of a novel histone deacetylase HDAC10. *J Biol Chem* 2002;277:3350-6.
 22. Li Y, Seto E. HDACs and HDAC inhibitors in cancer development and therapy. *Cold Spring Harb Perspect Med* 2016;6:a026831.
 23. Islam MM, Banerjee T, Packard CZ, Kotian S, Selvendiran K, Cohn DE, et al. HDAC10 as a potential therapeutic target in ovarian cancer. *Gynecol Oncol* 2017;144:613-20.
 24. Géraldy M, Morgen M, Sehr P, Steimbach RR, Moi D, Ridinger J, et al. Selective inhibition of histone deacetylase 10: hydrogen bonding to the gatekeeper residue is implicated. *J Med Chem* 2019;62:4426-43.
 25. Hsieh YL, Tu HJ, Pan SL, Liou JP, Yang CR. Anti-metastatic activity of MPTOG211, a novel HDAC6 inhibitor, in human breast cancer cells in vitro and in vivo. *Biochim Biophys Acta Mol Cell Res* 2019;1866:992-1003.
 26. Herbst-Gervasoni CJ, Steimbach RR, Morgen M, Miller AK, Christianson DW. Structural basis for the selective inhibition of HDAC10, the cytosolic polyamine deacetylase. *ACS Chem Biol* 2020;15:2154-63.
 27. Morgen M, Steimbach RR, Géraldy M, Hellweg L, Sehr P, Ridinger J, et al. Design and synthesis of dihydroxamic acids as HDAC6/8/10 inhibitors. *ChemMedChem* 2020;15:1163-74.
 28. Herbst-Gervasoni CJ, Christianson DW. X-ray crystallographic snapshots of substrate binding in the active site of histone deacetylase 10. *Biochemistry* 2021;60:303-13.
 29. Herp D, Ridinger J, Robaa D, Shinsky SA, Schmidtkunz K, Yesiloglu TZ, et al. First fluorescent acetylspermidine deacetylation assay for HDAC10 identifies selective inhibitors with cellular target engagement. *Chembiochem* 2022;23:e202200180.
 30. Wang C, Lin Y, Zhu H, Zhou Y, Mao F, Huang X, et al. Efficacy and safety profile of histone deacetylase inhibitors for metastatic breast cancer: a meta-analysis. *Front Oncol* 2022;12:901152.
 31. Zeyen P, Zeyen Y, Herp D, Mahmoudi F, Yesiloglu TZ, Erdmann F, et al. Identification of histone deacetylase 10 (HDAC10) inhibitors that modulate autophagy in transformed cells. *Eur J Med Chem* 2022;234:114272.
 32. Kumar A, Swami S, Sharma NK. Distinct DNA metabolism and anti-proliferative effects of goat urine metabolites: an explanation for xeno-tumor heterogeneity. *Curr Chem Biol* 2020;14:48-57.
 33. Kumar A, Patel S, Bhatkar D, Sarode SC, Sharma NK. A novel method to detect intracellular metabolite alterations in MCF-7 cells by doxorubicin induced cell death. *Metabolomics* 2021;17:3.
 34. Raj AK, Lokhande KB, Prasad TK, Nandangiri R, Choudhary S, Pal JK, et al. Intracellular ellagic acid derived from goat urine DMSO fraction (GUDF) predicted as an inhibitor of c-Raf kinase. *Curr Mol Med* 2024;24:264-79.
 35. Raj AK, Upadhyay V, Lokhande KB, Swamy KV, Bhonde RR, Sarode SC, et al. Free fatty acids from cow urine DMSO fraction induce cell death in breast cancer cells without affecting normal GMSCs. *Biomedicines* 2023;11:889.
 36. Morris GM, Goodsell DS, Halliday RS, Huey R, Hart WE, Belew RK, et al. Automated docking using a Lamarckian genetic algorithm and an empirical binding free energy function. *J Comput Chem* 1998;19:1639-62.
 37. National Center for Biotechnology Information. PubChem Compound Summary for CID 162679241. <https://pubchem.ncbi.nlm.nih.gov/compound/162679241> (Accessed July 4, 2022).
 38. Trott O, Olson AJ. AutoDock Vina: improving the speed and accuracy of docking with a new scoring function, efficient optimization, and multithreading. *J Comput Chem* 2010;31:455-61.
 39. Schyman P, Liu R, Desai V, Wallqvist A. vNN web server for ADMET predictions. *Front Pharmacol* 2017;8:889.
 40. Daina A, Michielin O, Zoete V. SwissADME: a free web tool to evaluate pharmacokinetics, drug-likeness and medicinal chemistry friendliness of small molecules. *Sci Rep* 2017;7:42717.
 41. Huang Y, Hager ER, Phillips DL, Dunn VR, Hacker A, Frydman B, et al. A novel polyamine analog inhibits growth and induces apoptosis in human breast cancer cells. *Clin Cancer Res* 2003;9:2769-77.
 42. Vrijssen S, Besora-Casals L, van Veen S, Zielich J, Van den Haute C, Hamouda NN, et al. ATP13A2-mediated endolysosomal polyamine export counters mitochondrial oxidative stress. *Proc Natl Acad Sci USA* 2020;117:31198-207.
 43. Al-Habsi M, Chamoto K, Matsumoto K, Nomura N, Zhang B, Sugiura Y, et al. Spermidine activates mitochondrial trifunctional protein and improves antitumor immunity in mice. *Science* 2022;378:eabj3510.

44. Hiramatsu K, Takahashi K, Yamaguchi T, Matsumoto H, Miyamoto H, Tanaka S, et al. N(1),N(12)-Diacetylspermine as a sensitive and specific novel marker for early- and late-stage colorectal and breast cancers. *Clin Cancer Res* 2005;11:2986-90.
45. Kuwata G, Hiramatsu K, Samejima K, Iwasaki K, Takahashi K, Koizumi K, et al. Increase of N1, N12-diacetylspermine in tissues from colorectal cancer and its liver metastasis. *J Cancer Res Clin Oncol* 2013;139:925-32.
46. Wikoff WR, Hanash S, DeFelice B, Miyamoto S, Barnett M, Zhao Y, et al. Diacetylspermine is a novel prediagnostic serum biomarker for non-small-cell lung cancer and has additive performance with pro-surfactant protein B. *J Clin Oncol* 2015;33:3880-6.
47. Ou Y, Wang SJ, Li D, Chu B, Gu W. Activation of SAT1 engages polyamine metabolism with p53-mediated ferroptotic responses. *Proc Natl Acad Sci USA* 2016;113:E6806-12.
48. Fahrman JF, Vykoukal J, Fleury A, Tripathi S, Dennison JB, Murage E, et al. Association between plasma diacetylspermine and tumor spermine synthase with outcome in triple-negative breast cancer. *J Natl Cancer Inst* 2020;112:607-16.
49. Velenosi TJ, Krausz KW, Hamada K, Dorsey TH, Ambs S, Takahashi S, et al. Pharmacometabolomics reveals urinary diacetylspermine as a biomarker of doxorubicin effectiveness in triple negative breast cancer. *NPJ Precis Oncol* 2022;6:70.
50. Manni A, Grove R, Kunselman S, Aldaz CM. Involvement of the polyamine pathway in breast cancer progression. *Cancer Lett* 1995;92:49-57.
51. Iwata S, Sato Y, Asada M, Takagi M, Tsujimoto A, Inaba T, et al. Anti-tumor activity of antizyme which targets the ornithine decarboxylase (ODC) required for cell growth and transformation. *Oncogene* 1999;18:165-72.
52. Casero RA Jr, Marton LJ. Targeting polyamine metabolism and function in cancer and other hyperproliferative diseases. *Nat Rev Drug Discov* 2007;6:373-90.
53. Zhu Q, Huang Y, Marton LJ, Woster PM, Davidson NE, Casero RA Jr. Polyamine analogs modulate gene expression by inhibiting lysine-specific demethylase 1 (LSD1) and altering chromatin structure in human breast cancer cells. *Amino Acids* 2012;42:887-98.
54. Murray-Stewart TR, Woster PM, Casero RA Jr. Targeting polyamine metabolism for cancer therapy and prevention. *Biochem J* 2016;473:2937-53.
55. Tamari K, Konno M, Asai A, Koseki J, Hayashi K, Kawamoto K, et al. Polyamine flux suppresses histone lysine demethylases and enhances *ID1* expression in cancer stem cells. *Cell Death Discov* 2018;4:104.
56. Hibino S, Eto S, Hangai S, Endo K, Ashitani S, Sugaya M, et al. Tumor cell-derived spermidine is an oncometabolite that suppresses TCR clustering for intratumoral CD8⁺ T cell activation. *Proc Natl Acad Sci USA* 2023;120:e2305245120.